Copyright © 1996 Elsevier Science Ltd
Paper No. 210. (quote when citing this article)
Eleventh World Conference on Earthquake Engineering
ISBN: 0 08 042822 3

RESEARCH ON THE NEW CONCRETE STRUCTURE REINFORCED WITH STEEL PLATES

FURUTA TOMOKI*, YAMAMOTO YASUTOSHI**

* Technology Research Center, Yahagi Construction Co., Ltd,
19-7, Aoi 3chome, Higashi-ku, Nagoya, 461. Japan
** Department of Architecture, Faculty of Engineering, Shibaura Institute of Technology,
9-14, Shibaura 3chome, Minato-ku, Tokyo, 108. Japan

ABSTRACT: In recent years, Japan has been experiencing a severe shortage of technical laborers engaged in housing production and supply, mainly in urban areas where construction activities are aggressively carried out. The tight labor supply is a structural problem due to the combination of diminishing of young entrants and aging of active laborers. Given the possibility of declining population of technical laborers leading to deterioration of overall construction skills, the situation is becoming critical.

Work has been carried out on the research and development of a new construction method as one medium-rise and high-rise housing production and supply system to address the worsening technical labor shortage and the resultant rise in construction cost and extension of construction period and to meet the advancing and diversifying needs of consumers and the mounting requirements of new times.

The new construction method substitutes steel plates for reinforcing bars as members to resist the bending and shearing forces of reinforced concrete as one method for simplifying the structural system and is called the PLRC construction.

KEYWORDS: PLRC construction, steel plate, beam specimen, experiment, high ductility

1 INTRODUCTION

The PLRC construction is characterized by its members. The cross section of each concrete column is cross shaped. A cross-shaped steel plate is placed at the center of the column, and a flat steel plate is arranged at each side of the column, as shown in Fig.1. The cross section of each concrete beam is rectanglar. The beam is as wide as the column is thick and has a full-web steel plate arranged as shown in Fig.2. Spiral annealing wire reinforcement is placed around each steel plate in the column and beam to prevent the separation of the steel plate from the concrete in the column and beam, increase the bond force of the steel plate to the concrete, enhance the confining effect of the concrete, and prevent the buckling of the steel plate.

The PLRC construction is a pure frame structure without shear walls. The absence of shear walls allows addition and rebuilding to be made without structural damage and the space to be fully utilized. The columns, beams, and walls are built to the same width to provide a interior space like a wall structure without any protrusions.

Column and beam members are each prefabricated, and half-precast concrete slabs are used as floor members. The column and beam members are connected by the center joint method whereby high-tension bolts are used to make the joint. The joint and floor concrete are cast together to form an integral structure as shown in Fig.3.

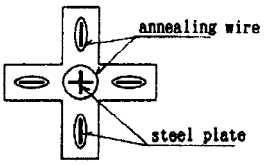

Fig.1 Column

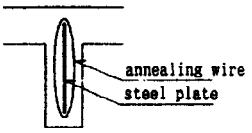

Fig.2 Beam

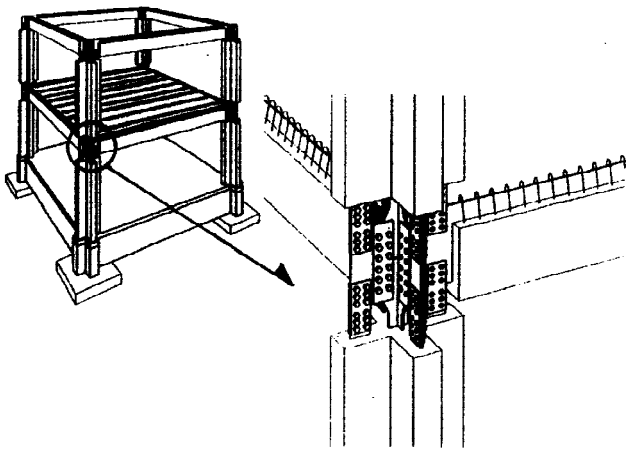

Fig.3 Center joint method

This study performed the preliminary design of a 30-story building of the PLRC construction, experimented with 1/2-scale beam specimens, investigated the dynamic properties of the PLRC construction, and verified the guaranteed strength of the PLRC construction.

2 EXPERIMENTAL METHODS

2.1 Specimens

A 30-story building was preliminarily designed, and beam experiments were conducted using 1/2-scale beam specimens (beam depth of 450 mm, beam width of 175mm, specimen length of 2,700 mm, and shear span length of 1,100 mm). Three types of beam specimens of the same concrete cross section but of different steel plate shape were used in the experiments. One type (G350) had a single 16-mm thick and 350-mm wide steel plate, another (G150) had two 16-mm thick and 150-mm wide steel plates, and the other (G125) had two 16-mm thick and 125-mm wide steel plates, as shown in Fig.4. Spiral annealing wire was placed around each steel plate at the pitch of 25 mm. A loading stub was provided at the center of each specimen by considering the distance from the column face to the center of the beam and assuming the yielding of the beam edges.

Strain gages were attached to each specimen as shown in Fig.4 to determine the load-strain relationship and confirm the bond between the steel plate and concrete. The strain gages were attached to the steel plate and concrete surfaces at 100-mm and 200-mm intervals from the center of the beam, respectively.

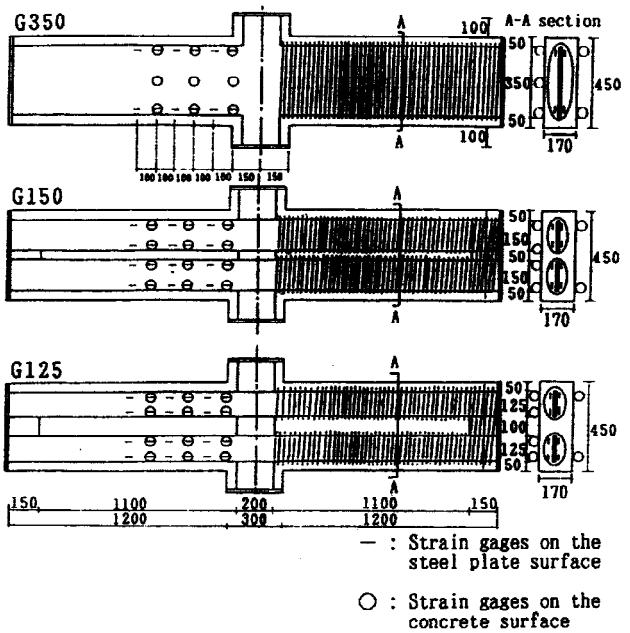

Fig.4 Specimens

The properties of the materials used in the experiments are listed in Tables 1 and 2. Young's modulus assumed in the analysis of the experimental results discussed later is 2.1×10^5MPa for the steel plates, 2.1×10^5MPa for the spiral annealing wire, 2.3×10^4 MPa for the concrete .

Table 1. Properties of steel

Specimens	Sectional form (mm)	Section area (mm^2)	Yielding stress (kN)	Maximum stress (kN)	Yielding unit stress (MPa)	Maximum unit stress (MPa)	Young's modulus (MPa)
Steel plate	15.5(Thickness) 40.0(Width)	620.0	205.9	313.1	331.2	504.7	2.1×10^5
Annealing wire	5.0(Diameter)	19.6	3.4	6.1	175.4	309.7	2.1×10^5

Table 2. Properties of concrete

Specimens	Test piece number	Maximum unit stress (MPa)	Young's modulus (MPa)
G350	No.1	37.3	2.12×10^4
	No.2	39.3	2.32×10^4
	No.3	41.2	2.54×10^4
	Average	39.3	2.33×10^4
G150 G125	No.1	43.1	2.39×10^4
	No.2	44.0	2.25×10^4
	No.3	44.9	2.26×10^4
	Average	44.0	2.30×10^4

2.2 Loading

The loading apparatus is schematically illustrated in Fig.5. The specimen was repeatedly and alternately loaded by the two oil jacks at the center of the frame. The specimen was supported at the middle of the beam depth at each end by a special pin and roller device so that no secondary frictional force should develop at the support due to bending. The deflection of the beam was determined by measuring the relative displacement of the supports with a device installed at the center of the specimen.

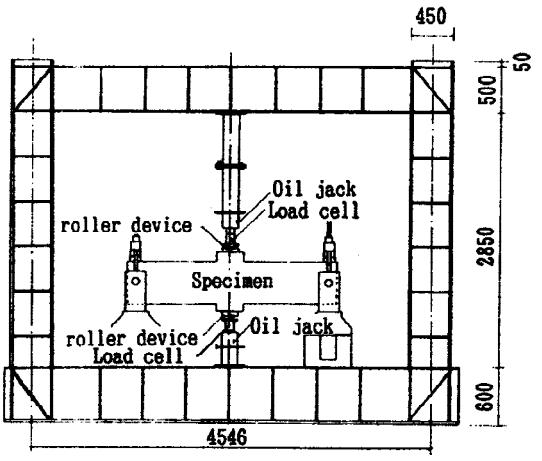

Fig.5 Loading apparatus

The loading program consisted of applying a small elastic load to the specimen for one cycle and then deforming the specimen by changing the angle of rotation in increasing order of 1/1000, 1/500, 1/250, 1/120, 1/80, 1/60, 1/40, 1/30, and 1/20 .

3 EXPERIMENTAL RESULTS and DISCUSSION

3.1 Cracks

The final cracks observed in the specimens are shown in Fig.6. The G350 specimen had bending cracks close to the support positions and developed few shear cracks. The cracks were very fine except for the large bending cracks near the support positions. There cracks may be explained by the fact that the full-web steel plate in the G350 specimen carried almost all of the shearing force encountered. The G150 specimen showed some shear cracks, but the cracks did not appreciably extend in the final stage. This result suggests that the two steel plates in the G150 specimen carried the shearing force, not to the same extend as observed in the G350 specimen, but to a considerable extent. The G125 specimen had more shear cracks than the G150 specimen. This is probably because the shearing force was not totally carried by the steel plates and was also carried by the concrete. After the compressive failure of the concrete in each specimen, the spiral annealing wire apparently confined the concrete and prevented the buckling of the steel plate or plates. The buckling phenomenon was not confirmed, therefore.

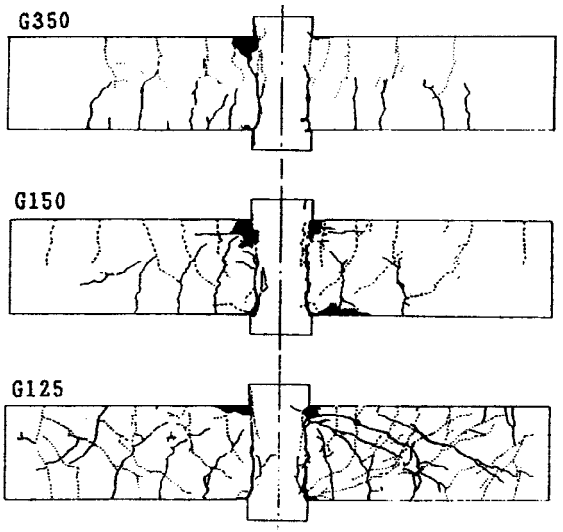

Fig.6 The final cracks

3.2 Relationship between load and deformation

The relationship between load and deformation is shown in Fig.7. The letters M,S,C, and P on the hysteresis loops indicate the occurrence of bending cracks in the concrete, occurrence of shear cracks in the concrete, occurrence of compressive cracks in the concrete, and onset of yielding in the plate edge, respectively. The numbers on the hysteresis loops are cycle numbers.

The hysteresis loops of each specimen are nearly spindle shaped and exhibit characteristics close to the stable propertics of steel framed reinforced concrete beams. The specimens are also equal in the positions of the letters M,S,C, and P for the same number of cycles and show similar fracture stages.

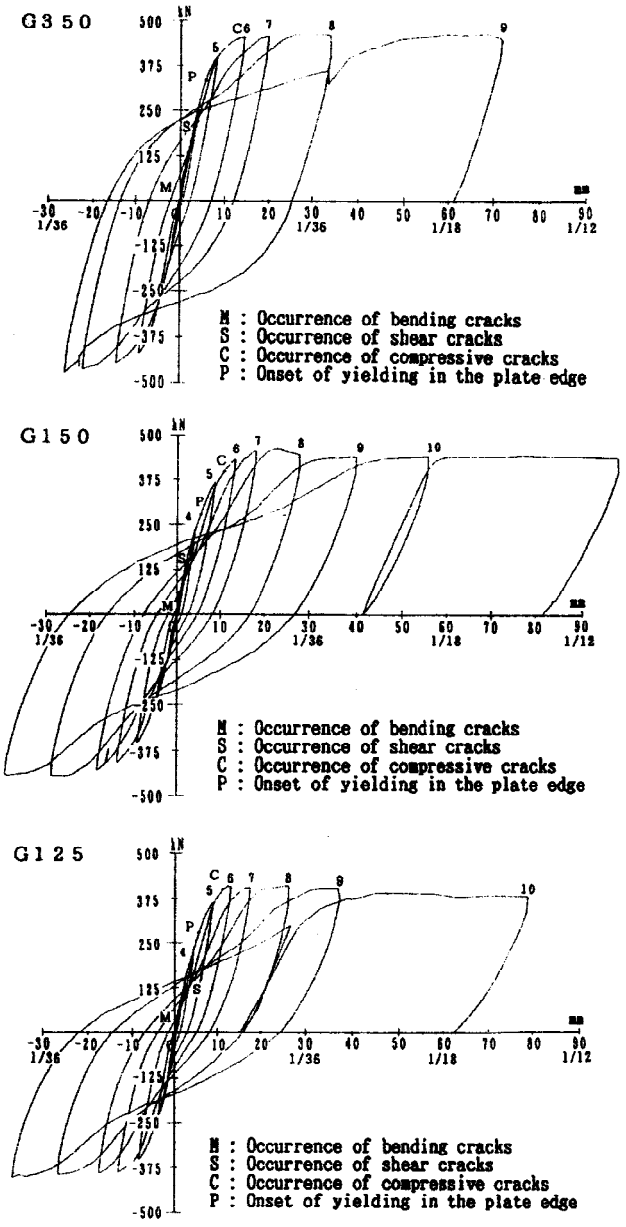

Fig.7 The relationship between load and deformation

The strength of the specimens increases after the yielding of the plate edges. After the occurrence of compressive cracks in the concrete, the specimens did not increase in strength, but advanced in deformation. The specimens did not decline in strength until they were deformed to the angle of rotation of 1/20 or more. This attests to the high toughness of the specimens.

4 ANALYSIS of EXPERIMENTAL RESULTS

This chapter analyzes the experimental results and proposes beam strength equations. Since the experimental results confirmed that the specimens predominantly failed by bending fracture, ultimate bending strength equations are studied here.

4.1 Strain state of steel plates

Figure 8 shows the strain distribution of the steel plates when loaded to the maximum level for 6 cycles. The neutral axis at the center of the been is on the compressive side (upper part of the beam) and in almost the same position for the three specimens. With the G350 specimen with a single steel plate, the steel plate edges yielded on the tensile side (lower part of the beam), and the yield region expanded along the bending stress curve. The G150 and G125 specimens with two steel plates each had the yield strain concentrated at the center of the beam. There was no yield region expansion as observed in the G350 specimen, and the yield region fell within the elastic region.

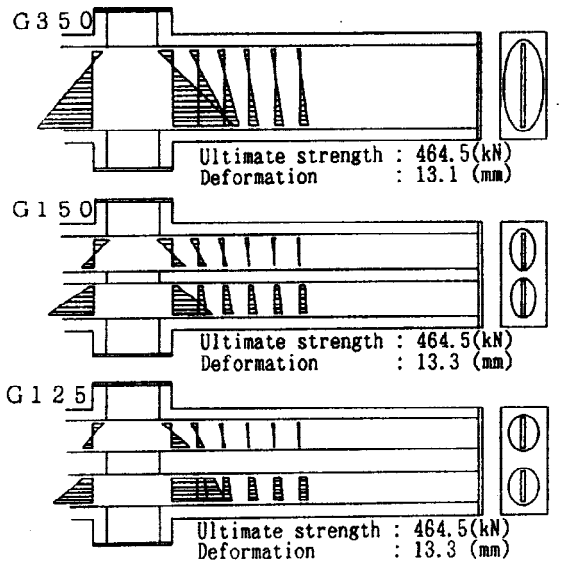

Fig.8 Strain state of steel plates

When the steel plate on the tension side is subjected to in-plane bending tensile force, the bond strength of the steel plate surface in the position a in Fig.9 cannot be expected, but the compressive friction between the steel plate and concrete in the position b is expected to work to prevent the yield region from expanding. Accordingly, it is judged possible to expect the composite effect of the concrete and steel plate from the beam.

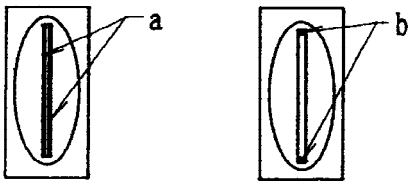

Fig.9 Position a & b

4.2 Load carrying capacity (ultimate bending strength)

The beam strength equations were derived by reference to the strain state of the steel plate as described below. The stress distribution of the concrete and steel plate in the beam cross section is assumed as illustrated in Fig.10. The average compressive stress of the concrete is put at 85% of the concrete strength and is considered to be distributed in rectangular from as show in Fig.10. The steel plate on the upper compressive side is assumed to completery yield in tension, while the steel plate on the upper compressive side is assumed to completely yield across the neutral axis.

Since the resultant force of the concrete and steel plate on the compressive side (C_c+C_s) is equal to the resultant force of the steel plate on the tensile side (T_1+T_2), the position of the neutral axis (X_n) is given by

$$X_n = 2t\times\sigma_y\times(h+a)/(2t\times\sigma_y+0.85\times B\times F_c) \quad (1)$$

The yield moment (M_y) is obtained as the sum of moments about the neutral axis of the cross section.

$$M_y = 0.425\times X_n\times B\times F_c\times(D-X_n)+0.5t\{\sigma_y\times((X_n-a)\times(D-X_n-a)+h(D-h-2a)-e(e+b)\} \quad (2)$$

where

$$e = a+h-X_n$$

The values thus calculated are taken as theoretical values 1 and compared with the experimental values in Table 3. The theoretical values 1 closely agree with the experimental values.

If the column has the axial force N, the neutral axis position and yield moment are obtained by a procedure similar to that for the beam by assuming $C_c+C_s+N=T_1+T_2$.

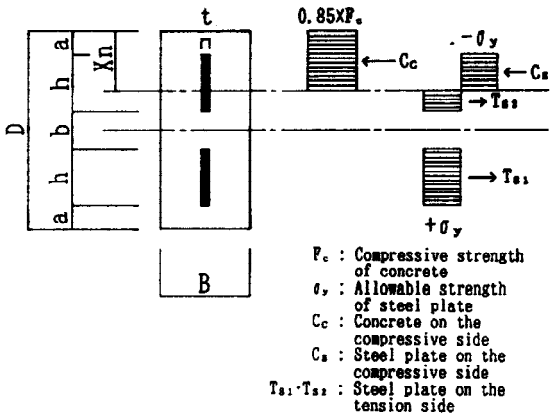

Fig.10 The stress distribution of the concrete and steel plate in the beam cross section

Table 3. Comparison between experimental and analytical values

Specimens	The experimental values (kN)	The theoretical values 1 (kN)	The theoretical values 2 (kN)	Experiment / Values 1	Experiment / Values 2
G350	464.5	460.6	455.7	1.01	1.02
G150	453.7	437.1	426.3	1.04	1.06
G125	400.8	368.5	357.7	1.09	1.12

4.3 Elasto-plastic deflection of beam

The relationship between the moment(M) and curvature(Φ) of the beam cross section was obtained by using the properties of the materials listed in Table 1 and 2. The deflection of the beam in the elasto-plastic region was analyzed by using the method of solution that extends Mohr's theorem to the plastic region and was compared with the experimental values. The elastic deformation of the beam was considered only as shear deformation.

4.3.1 Assumed conditions for materials

The stress-strain relationship of the concrete is shown in Fig.11. The initial stiffness of the concrete is denoted by E_c (Table 2), the Ramberg-Osgood function is used up to the maximum load, and the E-function is assumed after the maximum load. The strain at the maximum load is put at 0.002.

4.3.2 Relationship between moment and curvature (M-Φ)

Assuming that the Navior hypothesis holds, the concrete and steel plate cross sections were divided into 40 and 28 parts, respectively, by the fiber model method. Figure 12 shows the results of the fiber model analysis. This analytical mathod determines the stress from the compressive and tensile strain distributions by holding a given radius of curvature constant and changing the neutral axis. The position of the neutrel axis is obtained by the trial-and-error method so that the compressive resultant becomes equal to the tensile resultant. The relationship between the moment and curvature at a given radius of curvature is determined accordingly. Since the G350 specimen with a single steel plate has the position of the neutral axis situated closer to the cross-sectional center than the other two specimens, it had higher compressive strain and lower strength for the same curvature. Its strength started to decrease from $\Phi=2X10^{-4}$.

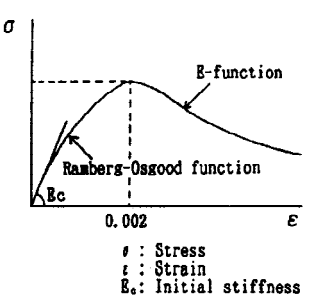

Fig.11 The stress-strain relationship of the concrete

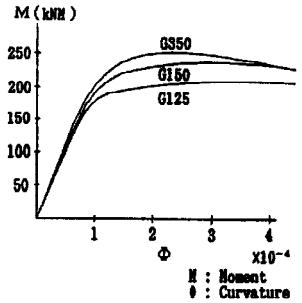

Fig.12 The results of the fiber model analysis

4.3.3 Deflection of beam

Figure 13 shows the curvature-load distribution obtained by the method of extending Mohr's theorem to the prastic region. The relationship between the moment and curvature is the same as shown in Fig.12. Since the steel plate of the stub located at the center of the specimen and jointed to the beam steel plate, it was assumed to have the same strain as the beam steel plate. Elastic deformation was considered as shear deformation.

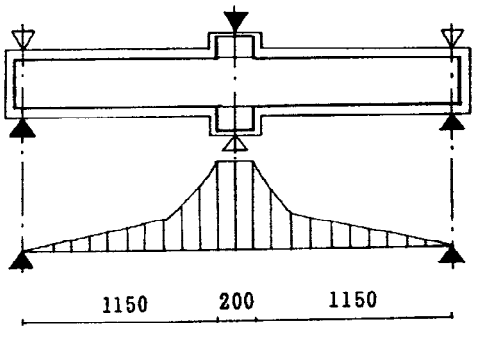

Fig.13 The curvature-load distribution

4.4 Comparison between experimental and analytical values

Figure 14 shows the relationship between the load and deformation measured in the experiments (solid line) and the relationship between the load and deformation calculated by the above method (dotted line). The measured and calculated values almost agree until the yielding of the steel plate for the G350 specimen with a single steel plate. As the load increases, some errors occur between the measured and calculated values for the G150 and G125 specimens with two steel plates each, probably under the influence of shear cracks. The calculated values will more closely agree with the measured values if the effect of shear cracks is taken into account. The calculated maximum strength agree well with the measured maximum strength. These analytical values are taken as theoretical values 2 and are given in Table 3. The theoretical values 2 were smaller than the theoretical values 1 on the whole.

5 CONCLUSIONS

Table 4 shows the experimental results. When its steel plate width is large, the specimen is high in all of the bending cracking load, shear cracking load, steel plate yielding load, and compressive cracking load. Each specimen exhibits bending yielding type failure characteristics and has little loss of yield after the yielding of the steel plate or plates. When deformed to a minimum angle of rotation of 1/18 (or a minimum ductility factor of 14), the specimens retained over 80% of the maximum strength and exhibited hysteretic characteristics close to those of a spindle-shaped hysteresis loop of high energy absorption. This means that the PLRC construction has a high ductility capacity and a very high seismic capacity.

Since the steel plate yield strain is concentrated at the center of the beam, large bending cracks occur at the joint between the steel plate and stub. The lower steel plate yields by tension, and the neutral axis is located in the upper steel plate. Thus, the theoretical values 1 [Eq.(2)] can be applied as approximate solutions. the theoretical values 2, close to adjustable solutions obtained from the strength of the materials, are about 10% lower than the experimental values. This difference may be attributed to the assumptions of the Navier hypothesis and of the concrete stress and strain, among other factors. Calculated deflection will be made more realistic if plastic shear deformation is taken into account.

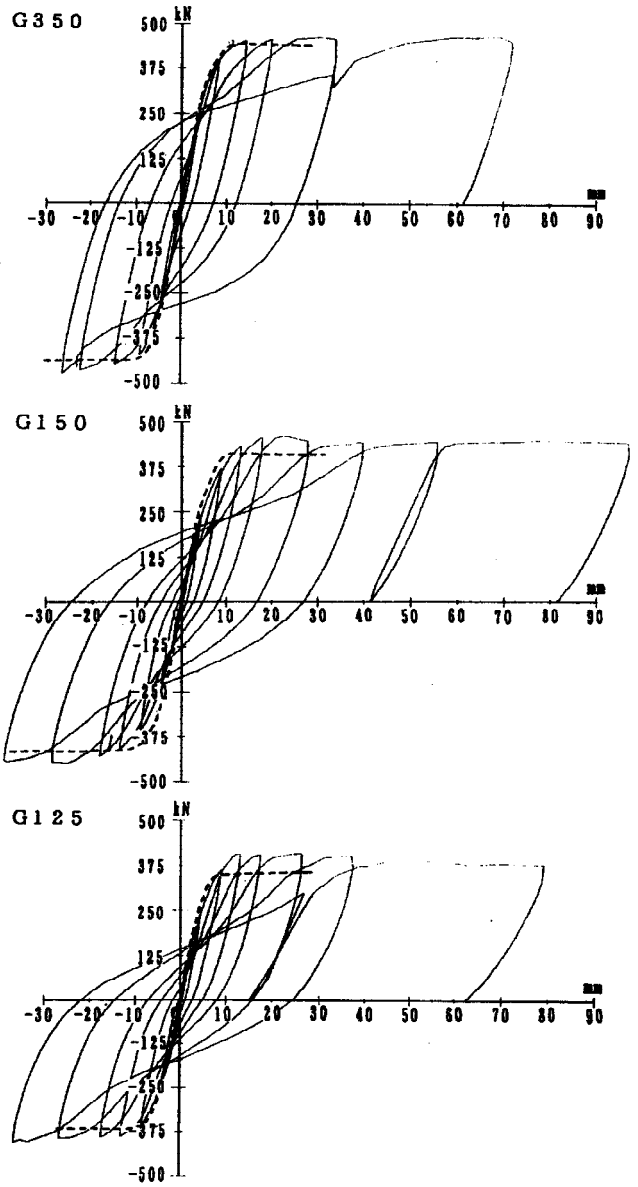

Fig.14 The relationship between the load and deformation by the theoretical values 2 (dotted line)

Table 4. Results of experiment

Specimens	Bending cracking load (kN)	Shear cracking load (kN)	Yielding load of steel plate (kN)	Compression failure load of concrete (kN)	Ultimate strength (kN)
G350	39.2	210.7	333.2	441.0	464.5
G150	32.3	132.3	274.4	406.7	453.7
G125	39.2	127.4	264.6	392.0	400.8

REFERENCES

Furuta, T. & Umemura, H. 1990. Proposed a new reinforced concrete system with steel plates. Transactions of the Architectural institute of Japan : 267-272

Furuta, T. & Yamamoto, Y. 1990. Development study of the Plates Reinforced Concrete Construction. Transactions of the Japan Concrete Institute Vol. 28